Quantum-confined Stark effects of exciton states in V-shaped GaAs/$Al_xGa_{1-x}As$ quantum wires

Kai Chang and J. B. Xia
National Laboratory for Superlattices and Microstructures, Institute of Semiconductors, Chinese Academy of Sciences, P.O. Box 912, Beijing 100083, People's Republic of China
(Received 5 January 1998)

Quantum-confined Stark effects are investigated theoretically in GaAs /$Al_xGa_{1-x}As$ quantum wires formed in V-grooved structures. The electronic structures of the V-shaped quantum wires are calculated within the effective mass envelope function theory in the presence of electric field. The binding energies of excitons are also studied by two-dimensional Fourier transformation and variational method. The blue Stark shifts are found when the electric field is applied in the growth direction. A possible mechanism in which the blueshifts of photoluminescence peaks are attributed to two factors, one factor comes from the asymmetric structure of quantum wire along the electric field and another factor arises from the electric-field-induced change of the Coulomb interaction. The numerical results are compared with the recent experiment measurement.
[S0163-1829(98)06727-7]

I. INTRODUCTION

Recently, the low-dimensional semiconductor structures, such as quantum wires [quasi-one-dimensional (Q1D) system] and quantum dots (Q0D system), have aroused much attention for potential application to high performance devices since they are theoretically predicted to offer superior optical and electrical characteristics.[1–3] There are many techniques to fabricate various real-quantum wires, such as electron beam lithography and etching, growth on the substrate with V grove, and selective growth on SiO_2 patterned GaAs (110) substrate, etc. In general, there are two kinds of quantum wires. In the first kind of quantum wires, one material is embedded in another material. The second kind of quantum wires has a free surface on the entire side or part of the side in the air, which are formed by lithography and chemical etching. In this field, recent investigations focus on the V-shaped and T-shaped quantum wires.[4–10] These quantum wires share desirable optical properties (the enhancement of exciton binding energy and a small linewidth) for device applications.

Electric field applied perpendicularly to the layer of quantum wells can change significantly the optical properties [absorption, reflection, and photoluminescence (PL)] of semiconductor quantum-well structures. This effect is referred to as the quantum-confined Stark effect (QCSE); it has been studied extensively in the past decades[11–14] for application of optical switches and modulators. Theoretically, the quantum wires and quantum dots can offer the advantage of lower switching energy and enhanced oscillator strength over the quantum well. Therefore, the low-dimensional systems are promised for low-energy optoelectronics devices. Recently, the electro-optical properties has been investigated in V-shaped GaAs/$Al_xGa_{1-x}As$ quantum wires by PL experiments; blueshifts of PL peak under electric field was observed.[15]

It is necessary to calculate the energy eigenvalues of the real quantum-wire structure for design of the device. Inoshita and Sakaki[16] calculated the electronic structure of a ridge wire recently. They modeled the confined potential by an approximate analytic expression and employed a coordinate transformation such that the interface was planar.[17] The finite-element method was applied to obtain the confinement energies. Goldoni *et al.*[18] and Rossi and Molinari[19] developed a numerical method in which the envelope function was expanded in terms of the plane-wave basis and calculated the electronic structures of realistic V-shaped quantum wire. In the above mentioned papers, the Coulomb interaction between electron and hole was not taken into account. On the other hand, there are several theoretical works on the exciton state in some ideal quantum wires. Binding energies of exciton in GaAs/$Al_xGa_{1-x}As$ rectangular quantum wires were investigated by Brown and Spector[20] and Degani and Hipolito.[21] Banyai *et al.*[22] also calculated the exciton and biexciton ground-state binding energies assuming infinite confining potential. Shik[23] considered a dielectric cylinder with the dielectric constant $\epsilon \gg 1$ placed in vacuum. He calculated the impurity bound-state binding energy, and found that image charge causes an obvious increase in binding energy. Very recently, Xia and Cheah[24] investigated the exciton states in an isolated quantum wire in which the valence-band mixing effect is taken into account. They found the exciton binding energy in the isolated wire is about ten times larger than that in the quantum well. Benner and Haug[25] assumed a parabolic confining potential and investigated the QCSE in a quantum wire. Hartree correction and the exchange-correlation effects are both taken into account. They found the blueshifts of PL peaks for low fields.

In this paper, we apply a numerical method to calculate the exciton states in real quantum-wire structures formed in V-grooved substrate in the presence of an electric field. The binding energies of excitons are studied by using two-dimensional Fourier transformation and the variational method. A possible mechanism of blueshifts of PL peaks is proposed. It arises from the two aspects; one comes from the asymmetric geometry of wire cross section and another results from the electric-field-induced change of Coulomb interaction. The former is different from the result of Benner and Haug's study. In Sec. II, the theory of the QCSE in V-shaped quantum wires is presented. In Sec. III, the nu-

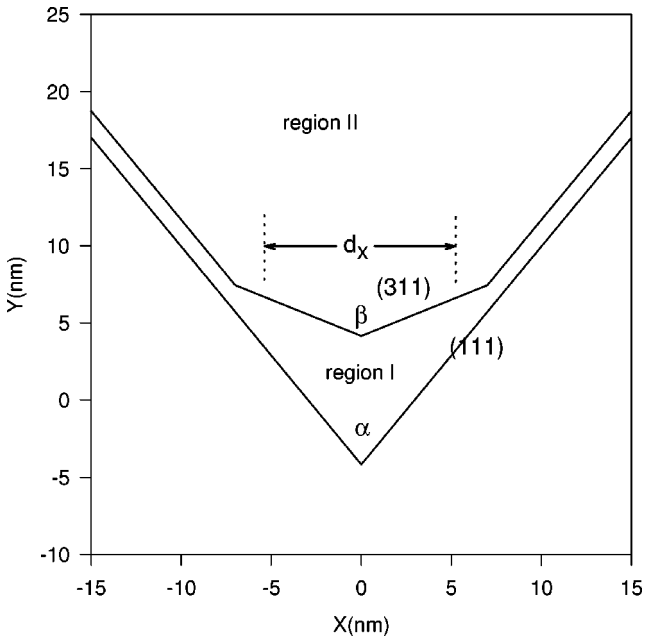

FIG. 1. Typical cross section of a V-shaped quantum wire derived from TEM micrographs; the frame of figure denotes the 2D periodic cell.

merical results are given and discussed. Finally, we give the conclusion in Sec. IV.

II. THEORY

We consider a quantum-wire sample formed in a V-grooved substrate, which is grown epitaxially by selective growth technique. A sketch of the sample is shown in Fig. 1. Electron and hole are confined in the xy plane and move freely along the wire direction (z axis). After separation of center-of-mass and relative motion in the z direction, the Hamiltonian for the system can be written as

$$H = H_e + H_h + V_{eh} + V_F, \tag{1}$$

$$H_e = -\nabla_e \frac{\hbar^2}{2m_e^*(x,y)}\nabla_e + V_e(x,y), \tag{2}$$

$$H_h = -\nabla_h \frac{\hbar^2}{2m_h^*(x,y)}\nabla_h + V_h(x,y), \tag{3}$$

$$V_{eh} = -\frac{e^2}{4\pi\epsilon_0\epsilon\sqrt{z^2+\rho^2}}, \tag{4}$$

$$V_F = \pm eFy, \tag{5}$$

where $\rho = \sqrt{(x_e - x_h)^2 + (y_e - y_h)^2}$ is the relative distance between electron and hole in the xy plane, e the electron charge, $\hbar$ the Planck constant, m_e^* (m_h^*) the effective mass of the electron (hole), F the strength of external electric field, and $V_F = \pm eFy$ the potential induced by the external static electric field. $V_e(x,y)$ [$V_h(x,y)$] is the confining potential for the electron (hole),

$$V_i(x,y) = \begin{cases} 0, & \text{Region I} \\ V_i, & \text{Region II,} \end{cases} \tag{6}$$

$$m^*(z) = \begin{cases} m_{iw}^*, & \text{Region I} \\ m_{ib}^*, & \text{Region II,} \end{cases} \tag{7}$$

where $i = e,h$ denotes electron or hole.

Electron and hole states in quantum wires are determined by the following Schrödinger equations respectively:

$$H_e\Psi_e = E\Psi_e, \tag{8}$$

$$H_h\Psi_h = E\Psi_h. \tag{9}$$

In general, these equations cannot be solved analytically due to complex geometry of a real quantum wire. In this paper, we expand the envelope function $\Psi_{e,h}$ in terms of a series of orthogonal complete bases that are composed of the plane waves in the x-y direction with periodic boundary condition. In quantum-well structures, Xia and Huang[26] and Zhu and Chang[27] have used the similar method to solve the Schrödinger equation in the presence of an external field. This method has also been applied to study the exciton optical transition in GaAs/Al_xGa_{1-x}As multiple quantum wells as a function of the field strength and proved successfully by comparison with experiment.[28] We extend the method to a two-dimensional case here; we assume that the barrier is so high and thick that it will bring in only a minor error by cutting the electric field at the barrier center and repeat it periodically. Thus, the potential in the presence of the electric field is

$$V_i(x+nL_x, y+mL_y) = V_i(x,y) = \begin{cases} \pm eFy, & \text{Region I} \\ V_i(x,y) \pm eFy, & \text{Region II.} \end{cases} \tag{10}$$

This assumption is both necessary for obtaining bound states in the presence of an external electric field and reasonable for long-lived quasibound states provide that the field strength is not too large. Following Ref. 25, we expand the electron or hole wave function in terms of normalized plane-wave basis set, respectively,

$$\Psi_{e,h}(x,y) = \frac{1}{\sqrt{L_xL_y}}\sum_{n,m} a_{nm} e^{ik_x x + iK_n x} e^{ik_y y + iK_m y} e^{ik_z z}. \tag{11}$$

Inserting Eq. (11) into Eq. (8), we obtained the secular equation

$$|H_{nm,n'm'} - E\delta_{nn'}\delta_{mm'}| = 0. \tag{12}$$

The elements of the Hamiltonian matrix can be given as

$$\langle H\rangle_{nm,n'm'} = \langle T\rangle_{nm,n'm'} + \langle V_{conf}\rangle_{nm,n'm'} + \langle V_F\rangle_{nm,n'm'}, \tag{13}$$

$$\langle T\rangle_{nm,n'm'} = -\int_{-L_x/2}^{L_x/2}\int_{-L_y/2}^{L_y/2} dxdy e^{-iK_m x} e^{-iK_n y}\nabla_i \times \frac{\hbar^2}{2m_i^*(x,y)}\nabla_i e^{iK_{m'}x} e^{iK_{n'}y}, \quad (14)$$

$$\langle V_{conf}\rangle_{nm,n'm'} = \int_{-L_x/2}^{L_x/2}\int_{-L_y/2}^{L_y/2} dxdy e^{iK_{nn'}x} e^{iK_{mm'}y} V_i(x,y), \quad (15)$$

$$\langle V_F\rangle_{nm,n'm'} = \begin{cases} 0 & m = m' \\ (-1)^{m-m'} \dfrac{\pm eFL_y}{2i(m-m')\pi}\delta_{nn'} & m \neq m', \end{cases} \quad (16)$$

where $+$ is for the hole while $-$ is for the electron, L_x and L_y are the periods of two-dimensional superlattice in the x-y plane, $K_n = n2\pi/L_x = nK_x$, $K_m = m2\pi/L_y = mK_y$, and n,m are integers. $K_{nn'}$ and $K_{mm'}$ are

$$K_{nn'} = (n-n')\frac{2\pi}{L_x}, \quad (17)$$

$$K_{mm'} = (m-m')\frac{2\pi}{L_y}. \quad (18)$$

In principle, the dimensionality of the Hamiltonian matrix is infinite. Since we are only concerned with the ground states, we can truncate the series in Eq. (11). For V-shaped wires considered here, this series with 15 terms can give convergent results.

After we obtained the eigenvalues and wave functions of the electron and hole, respectively, we then take into account Coulomb interaction between the electron and hole. An approximate solution of Eq. (1) can be written in the form[29]

$$\Psi(x_e,y_e,x_h,y_h,z) = \Psi(x_e,y_e)\Psi(x_h,y_h)\varphi_{z,\gamma}(z), \quad (19)$$

where $\varphi_{z,\gamma}(z)$ is a variational wave function. By inserting Eq. (19) into Eq. (1), an effective one-dimensional equation for the relative motion along the wire direction is obtained:

$$\left[E_e + E_h - \frac{\hbar^2}{2\mu}\frac{d^2}{dz^2} + V_{eff}(z)\right]\varphi_{z,\gamma}(z) = E_\gamma \varphi_{z,\gamma}(z), \quad (20)$$

where $V_{eff}(z)$ is

$$V_{eff}(z) = \int\int\int\int dx_e dy_e dx_h dy_h |\Psi_e(x_e,y_e)|^2 \times |\Psi_h(x_h,y_h)|^2 V(x_e - x_h, y_e - y_h, z), \quad (21)$$

which is difficult to evaluate. In evaluating the interaction integration in Eq. (2), we employ a two-dimensional Fourier transform

$$\frac{1}{\sqrt{z^2+\rho^2}} = \frac{1}{2\pi}\int_{-\infty}^{\infty}\int_{-\infty}^{\infty} dq_x dq_y e^{-i\mathbf{Q}\cdot\rho}\frac{e^{-Q|z|}}{Q}, \quad (22)$$

where $Q = \sqrt{q_x^2 + q_y^2}$.

By using this transformation, we can integrate the all real-space variables analytically, which gives the following expression:

$$\begin{aligned} V_{eh} &= \frac{e^2}{2\pi}\sum_{n_e m_e} a^*_{n_e m_e}\sum_{n'_e m'_e} a^*_{n'_e m'_e}\sum_{n_h m_h} a^*_{n_h m_h}\sum_{n'_h m'_h} a^*_{n'_h m'_h}\int_{-\infty}^{\infty}\int_{-\infty}^{\infty} dq_x dq_y \frac{\sin(K^e_{nn'} - q_x)L_x/2}{K^e_{nn'} - q_x} \\ &\times \frac{\sin(K^e_{mm'} - q_y)L_y/2}{K^e_{mm'} - q_y}\frac{\sin(K^h_{nn'} - q_x)L_x/2}{K^h_{nn'} - q_x}\frac{\sin(K^h_{mm'} - q_y)L_y/2}{K^h_{mm'} - q_y}\frac{e^{-Q|z|}}{Q} \\ &= \frac{e^2}{2\pi}\sum_{n_e m_e} a^*_{n_e m_e}\sum_{n'_e m'_e} a^*_{n'_e m'_e}\sum_{n_h m_h} a^*_{n_h m_h}\sum_{n'_h m'_h} a^*_{n'_h m'_h}\int_0^{2\pi}\int_0^{\infty} d\theta dQ \frac{\sin[K^e_{nn'} - Q\cos(\theta)]L_x/2}{K^e_{nn'} - Q\cos(\theta)} \\ &\times \frac{\sin[K^e_{mm'} - Q\sin(\theta)]L_y/2}{K^e_{mm'} - Q\sin(\theta)}\frac{\sin[K^h_{nn'} - Q\cos(\theta)]L_x/2}{K^h_{nn'} - Q\cos(\theta)}\frac{\sin[K^h_{mm'} - Q\sin(\theta)]L_y/2}{K^h_{mm'} - Q\sin(\theta)}e^{-Q|z|}. \end{aligned} \quad (23)$$

The original four-dimensional integration has been reduced to the two-dimensional (2D) integration in the $\mathbf{k}$ space. The singularity $1/r, r\to 0$ in original real-space integration has been removed because $\lim_{x\to 0}\sin x/x = 1$.

A variational trial wave function φ_γ is taken as

$$\varphi_\gamma = \left(\frac{4\gamma}{\pi}\right)^{1/4} e^{-\gamma z^2}, \quad (24)$$

where γ is the variation parameter and it can be obtained by minimizing the energy

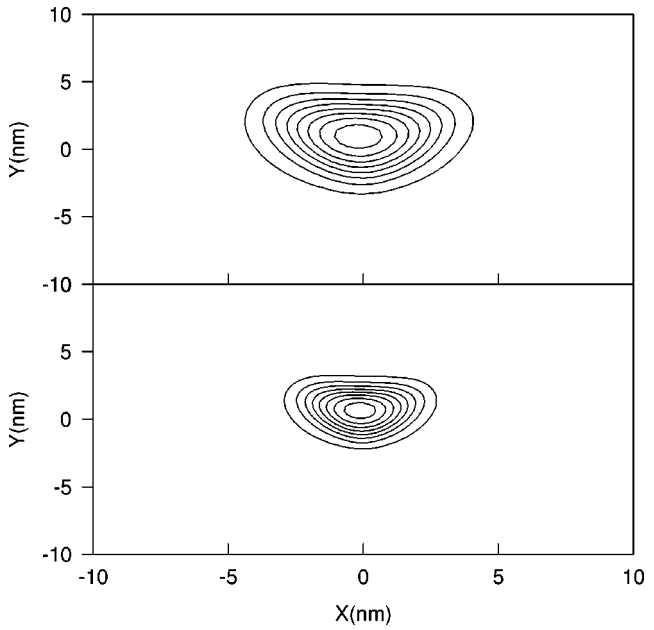

FIG. 2. Contour plot of the probability of electron (a) and heavy-hole (b) ground state $|\Psi_i|^2/\max|\Psi_i|$ in the absence of electric field ($i=e,h$). Lines denote 0.2, 0.4, 0.6, 0.8.

$$E_\gamma=\langle\varphi(z,\gamma)|-\frac{\hbar^2}{2\mu}\frac{d^2}{dz^2}+V_{eff}(z)|\varphi(z,\gamma)\rangle. \tag{25}$$

The binding energy of one-dimensional exciton is defined as

$$E_b=E_e+E_h-E, \tag{26}$$

where E_e and E_h are the single-particle energies of the electron and heavy hole, respectively, E is the ground-state energy of the one-dimensional exciton.

The Stark shift of the exciton is

$$\Delta E=E(F)-E(0)=\Delta E_q-\Delta E_b, \tag{27}$$

where $E(F)=E_e(F)+E_h(F)-E_b(F)$, ΔE_q is the difference of the quantized energies of the electron and hole without considering the excitonic effect.

III. NUMERICAL RESULTS AND DISCUSSIONS

In this section, we present numerical results of equations in Sec. II. We consider a V-shaped GaAs/$Al_{0.4}Ga_{0.6}As$ quantum wire. The typical 2D cross section of a V-shaped quantum wire is shown in Fig. 1. In the V-shaped wire the lower surface has a sharp corner with an angle between the sides $\alpha=70.6°$ [the angle between the (111) facets]; the upper surface also has a sharp corner with an angle between the sides $\beta=129.52°$ [the angle between the (311) facets]. The material parameters used in our calculations are $m_e^*=0.0665$, $m_h^*=0.45$, the dielectric constant $\epsilon=12.5$ for GaAs, $m_e^*=0.0997$, $m_h^*=0.45$, $V_e=313$ meV, $V_h=209$ meV, $\epsilon=10.9$ for $Al_{0.4}Ga_{0.6}As$.

The probabilities of the single-particle wave function $|\Psi_e(x,y)|^2$ and $|\Psi_h(x,y)|^2$ are shown in Figs. 2(a) and 2(b), respectively. The contours represent lines of constant probability $|\Psi_{e,h}(i)|^2/\max|\Psi_i(x,y)|^2=0.1,\quad 0.2,\ldots,0.8\quad (i=e,h)$. The contour lines show the distribution of the electron or hole in V-grooved quantum wire. From this figure, we can see that the electron (hole) on the ground-state level is localized in the bottom of the V-grooved quantum wire, and these contour lines mirror the cross-section structure of V-shaped wire. Obviously the localization of the hole is stronger than that of the electron. This arises from the fact that the effective mass of the hole is much heavier than that of the electron. Here we neglected the valence-band mixing effect. This approximation was taken in previous publications.[19] We are only concerned with the heavy-hole ground state since we will compare the transition energy between the ground states of the electron and heavy hole with the experiment. We compared the contours of the probability $|\Psi_h(x,y)|^2$ in the presence of electric field with that in the absence of electric field [Fig. 2(c)], and found that the contour lines vary slightly. It means that the electric-field-induced variation of the probability $|\Psi_h(x,y)|^2$ is very small. Thus, the separation between the electron and hole is also small in the quantum wire under the electric field. When an electric field is applied along the positive direction of the y axis, the hole is pushed to the top of the wire and the distribution of the hole becomes a little more extended compared to the case when the electric field is along the negative direction of the y axis.

In Figs. 3(a) and 3(b), we plot the energies of the electron and hole states as a function of electric field. The results show that the redshifts and blueshifts of the electron and hole levels are determined by the direction of the electric field applied on the sample. The Coulomb interaction between the electron and hole is not taken into account. The redshifts or blueshifts are caused by the asymmetric structure of the V-grooved quantum wire. In the bottom of the wire the confinement is stronger than that in the top of the wire. When the electron or hole is pushed to the bottom of the wire, the confinement is enhanced, and this enhancement results in raising of the energies of the electron and hole states. On the other hand, the electric field lowers the energies of the electron and hole states. There is a competition between the confinement and the electric field, which leads to the redshift or blueshift of the electron and hole levels. The insets show the transition energy between the electron and hole ground minus the band gap of GaAs as a function of electric field. From the results we find that the asymmetric character of energy shifts around zero electric field, and the asymmetric character is enhanced as the wire width increases. From these figures, we find that the asymmetric geometry of the wire cross section can cause the blueshifts of PL peaks. This mechanism is different from the mechanism proposed by Benner and Haug.[25]

Figure 4 shows the energies of the electron and hole states as functions of the width of the quantum wire in the presence of electric field. We find that the energies of the electron and hole states decrease rapidly as the wire width increases. From these figures the redshifts and blueshifts of the electron and hole levels are seen and determined by the direction of the electric field applied on the sample. In narrow wire, the confinement is much stronger than that in wide wire. Therefore the effect of the electric field on the energies of the electron and hole becomes more and more strong as the wire width increases. Since the hole effective mass is heavier than that of the electron, the electric-field-induced shifts of the

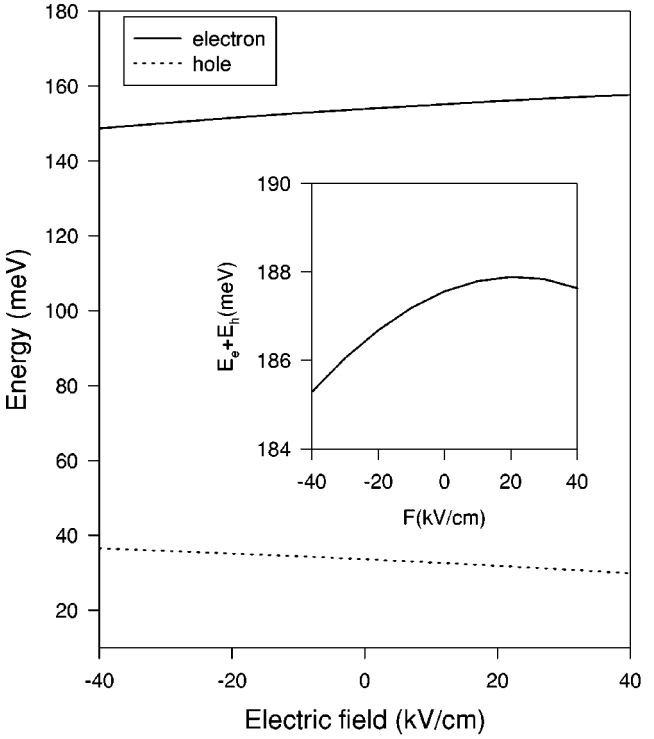

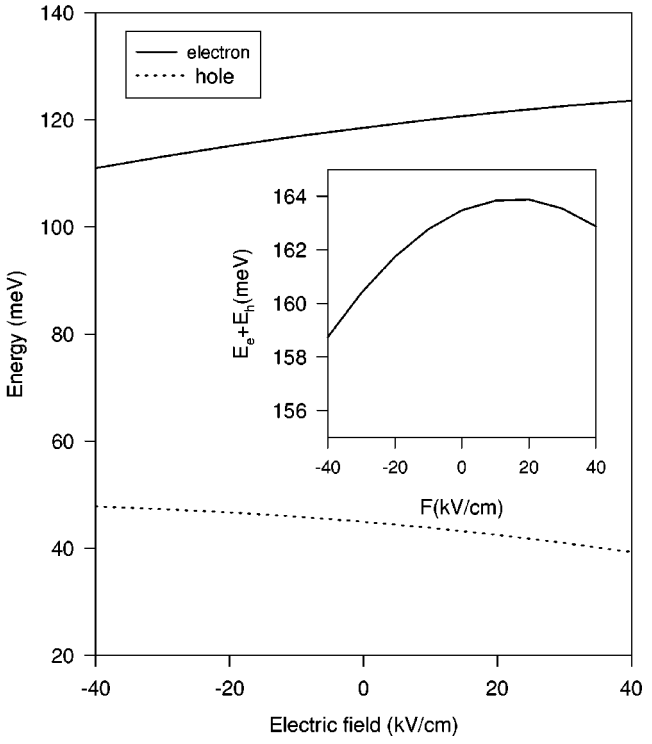

FIG. 3. The energies of the electron and hole states versus the strength of electric field for different wire width $d_x=8$ nm (a) 14 nm (b). The insets show E_e+E_h as functions of electric field.

hole energies are larger than those of the electron energies.

Figure 5 illustrates the effective Coulomb potential V_{eff} as a function of the relative distance between the electron and hole along the z axis with and without electric field. The effective Coulomb potential V_{eff} decreases rapidly as the relative distance $z=|z_e-z_h|$ increases. There is a slight difference of the effective Coulomb potential between the cases with and without electric field. When an electric field is applied on the sample, the electron and hole are separated in the direction of the electric field; thus the effective Coulomb potential V_{eff} decreases as the electric field increases. The binding energy of the exciton can be calculated from the effective Coulomb potential V_{eff} in Eq. (26). It is found that for $d_x=14$ nm, $E_b\approx 22$ meV. When an electric field $F=40$ kV/cm is applied on the sample, $E_b\approx 20$ meV for $d_x=14$ nm.

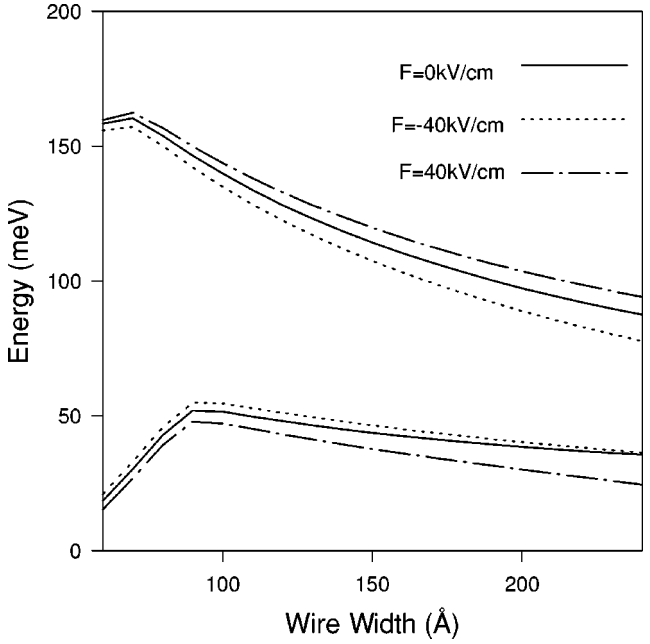

FIG. 4. The energies of electron and hole states versus the wire width under different bias $F=0$ kV/cm, ± 40 kV/cm.

In Fig. 6 we plot the Stark shifts of the exciton in a V-grooved quantum wire ($d_x=14$ nm); the inset shows the transition energy as a function of electric field. From this

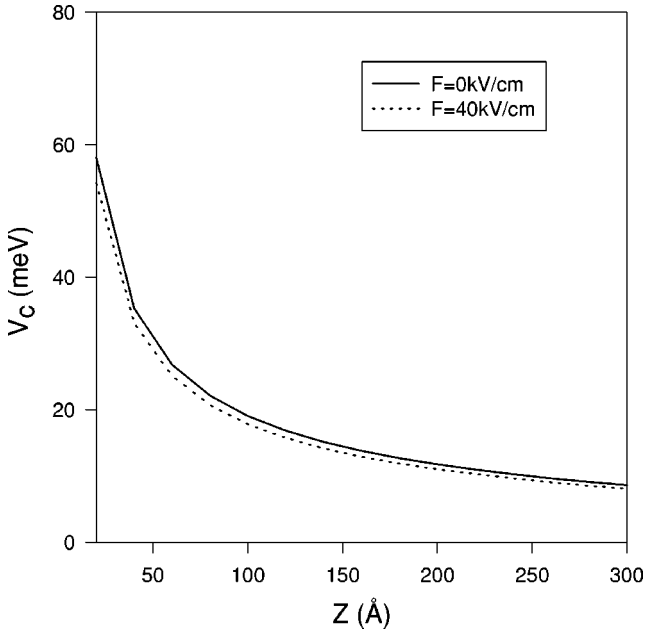

FIG. 5. The effective Coulomb interaction energy of ground state versus the relative distance between electron and hole for different electric field $F=0$, 40 kV/cm for wire width $d_x=14$ nm.

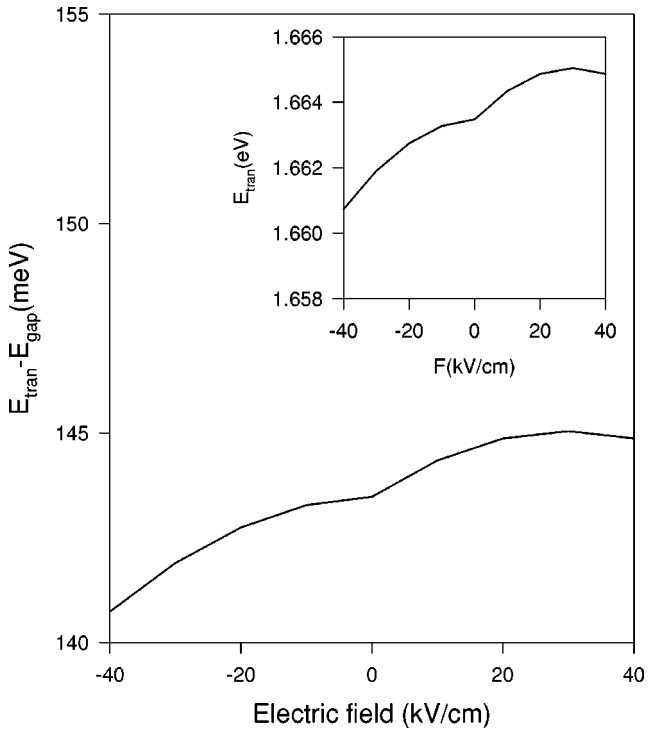

FIG. 6. The Stark shifts of the excitonic ground state in quantum wire ($d_x = 14$ nm) versus the strength of electric field.

figure we can find a blue Stark shift and a strong asymmetric shift around $F = 0$ kV/cm. The redshifts and blueshifts of the electron and hole levels have been shown in Figs. 3(a) and 3(b). Due to the asymmetry geometry of the cross section of the wire, and the difference of the effective masses and confinements of the electron and hole, the quantities of the redshifts and blueshifts of the electron and hole are different. Therefore, the asymmetry of the cross section of wire leads to the blueshifts of the PL peak even if the Coulomb interaction is not taken into account. The Stark shifts equal a difference of the electric-field-induced changes of the energies of the electron and hole quantized levels $\Delta E_q = \Delta E_e + \Delta E_h$ and the binding energies ΔE_b; $\Delta E = \Delta E_q - \Delta E_b$. In narrow wire the binding energy decreases drastically. The electric-field-induced change of the binding energy is larger than that of the quantized energies of the electron and hole; $|\Delta E_b| > |\Delta E_q|$. It leads to the blueshift of the PL peak in the quantum wire. From our calculation we also find that the electric-field-induced shifts of the electron and hole are not always redshifts [see Figs. 3(a) and 3(b)] they are influenced by the geometry of the cross section of the wire. When the electric field is applied along the positive direction of the y axis, the blueshift of the electron and hole energies E_q are found ($\Delta E_q > 0$). The electric-field-induced change of the binding energy of the exciton is another important factor. The binding energy of the exciton decreases with increasing electric field ($\Delta E_b < 0$). Since the electric field always separated the electron and hole, the separation leads to the reducing of the binding energy. Thus the blueshift is attributed to the two factors mentioned above. The first is the asymmetric cross section of wire, the second arises from the Coulomb interaction. Benner and Haug solved the Poisson and Schrödinger equations self-consistently. The many-body effects include the Hartree correction and exchange-correlation effects are considered in their calcualtion. The blueshifts of PL peaks in their study are attributed to the electric-field-induced changes of exciton binding energies. It is similar with the second factor in our calculation. Our numerical results can give the interpretation of the experimental measurement although the nummerical results are slightly smaller than experimental measurement. The difference between the theoretical results and the experimental measurement may come from the fact that the V-shaped wire structure taken in the calculation is an ideal model for realistic structure of quantum wire.

IV. CONCLUSION

In this paper, we presented a numerical approach that allows us to calculate the electronic structures of quantum wires in the presence of electric field, taking into account Coulomb interaction between the electron and hole together with realistic profiles of the confining potential. We studied the quantum-confined Stark shift effect in a V-grooved GaAs/$Al_{0.4}Ga_{0.6}As$ quantum wire, where the shape of the confinement region differs considerably from the ideal quantum wires in most of the previous investigation. We propose a mechanism of the blue Stark shifts observed in experiment. From our numerical results we find that the blue Stark shift is caused by the special geometry of the cross section of the quantum wire and the electric-field-induced decrease of the Coulomb interaction. The red and blue Stark shifts are determined by the direction of applied electric field. The binding energy of exciton is calculated by using a two-dimensional Fourier transformation and the variational method. The numerical results agree well with experimental measurement.[15]

ACKNOWLEDGMENT

This work was supported by the Chinese National Natural Science Foundation.

[1] Y. Arakawa and H. Sakaki, Appl. Phys. Lett. **40**, 939 (1982).
[2] H. Temkin, G. J. Dolan, M. B. Panish, and S. N. G. Chu, Appl. Phys. Lett. **50**, 413 (1987).
[3] Y. Arakawa, Solid-State Electron. **37**, 523 (1994).
[4] E. Kapan, D. M. Hwang, and R. Bhat, Phys. Rev. Lett. **63**, 430 (1989).
[5] M. Notomi, M. Naganuma, T. Tamamura, H. Iwamura, S. Nojima, and M. Okamoto, Appl. Phys. Lett. **58**, 720 (1991).
[6] S. Tsumamoto, Y. Nagamune, T. Nashioka, and Y. Arakawa, J. Appl. Phys. **71**, 533 (1992).
[7] M. Gailhanou, T. Baumbach, U. Marti, P. C. Silva, F. K. Reinhart, and M. Hegems, Appl. Phys. Lett. **62**, 1623 (1993).
[8] S. Tiwari, G. David Pettit, K. R. Milkove, F. Legones, R. J. Davis, and J. M. Woodall, Appl. Phys. Lett. **64**, 3536 (1994).

[9] R. Rinaldi, M. Ferrara, R. Cingolari, U. Marti, D. Martin, F. Morier-Gemoud, P. Ruterana, and F. K. Reinhart, Phys. Rev. B **50**, 11 795 (1994).
[10] M. Grundmann, V. Türck, J. Christen, E. Kapon, D. M. Hwang, C. Caneau, R. Bhat, and D. Bimberg, J. Nonlin. Opt. Phys. Mater. **4**, 99 (1995).
[11] D. A. B. Miller, D. S. Chemla, T. C. Damen, A. C. Gossard, W. Wiegmann, T. H. Wood, and C. A. Burrus, Phys. Rev. B **32**, 1043 (1985).
[12] G. Bastard, E. E. Mendez, L. L. Chang, and L. Esaki, Phys. Rev. B **28**, 3241 (1983).
[13] H. J. Polland, L. Schultheis, J. Kuhl, E. O. Göbel, and C. W. Tu, Phys. Rev. Lett. **55**, 2610 (1985).
[14] K. Köhler, H. J. Polland, and L. Schultheis, and C. W. Tu, Phys. Rev. B **38**, 5496 (1985).
[15] T. Arakawa, Y. Kato, F. Sogawa, and Y. Arakawa, Appl. Phys. Lett. **70**, 646 (1997).
[16] T. Inoshita and H. Sakaki, J. Appl. Phys. **79**, 269 (1996).
[17] D. Gershoni, H. Temkin, G. J. Dolan, J. Dunsmuir, S. N. G. Chu, and M. B. Panish, Appl. Phys. Lett. **53**, 995 (1988).
[18] G. Goldoni, F. Rossi, E. Molinari, A. Fasolino, R. Rinaldi, and R. Cingolani, Appl. Phys. Lett. **69**, 2965 (1996).
[19] F. Rossi and E. Molinari, Phys. Rev. Lett. **76**, 3642 (1996); Phys. Rev. B **53**, 16 462 (1996).
[20] J. W. Brown and H. N. Spector, Phys. Rev. B **35**, 3009 (1987).
[21] M. H. Degani and O. Hipolito, Phys. Rev. B **35**, 9345 (1987).
[22] L. Banyai, I. Galbraith, C. Ell, and H. Haug, Phys. Rev. B **36**, 6099 (1987).
[23] A. Shik, J. Appl. Phys. **74**, 2951 (1993).
[24] J. B. Xia and K. W. Cheah, Phys. Rev. B **55**, 1596 (1997).
[25] S. Benner and H. Haug, Phys. Rev. B **47**, 15 750 (1993).
[26] J. B. Xia and K. Huang, Acta. Phys. Sin. **37**, 1 (1988) [Chin. J. Phys. **9**, 303 (1989)].
[27] B. F. Zhu and Y. C. Chang, Phys. Rev. B **50**, 11 932 (1994).
[28] A. Blacha, H. Presting, and M. Cardona, Phys. Status Solidi B **126**, 11 (1984).
[29] Y. C. Chang, L. L. Chang, and L. Esaki, Appl. Phys. Lett. **47**, 1324 (1985).